Regulation of DLK1 by the maternally expressed miR-379/miR-544 cluster may underlie callipyge polar overdominance inheritance

Yun-Qian Gao[a,1], Xin Chen[a,1], Pei Wang[a], Lei Lu[a], Wei Zhao[a], Chen Chen[a], Cai-Ping Chen[a], Tao Tao[a], Jie Sun[a], Yan-Yan Zheng[a], Jie Du[b], Chao-Jun Li[a], Zhen-Ji Gan[a], Xiang Gao[a], Hua-Qun Chen[c], and Min-Sheng Zhu[a,b,2]

[a]State Key Laboratory of Pharmaceutical Biotechnology, Model Animal Research Center and Ministry of Education (MOE) Key Laboratory of Model Animal for Disease Study, Nanjing University, Nanjing 210061, China; [b]Innovation Center for Cardiovascular Disorders, Beijing Anzhen Hospital, Beijing 100029, China; and [c]School of Life Science, Nanjing Normal University, Nanjing 210009, China

Edited by Se-Jin Lee, Johns Hopkins University, Baltimore, MD, and approved September 29, 2015 (received for review June 11, 2015)

Inheritance of the callipyge phenotype in sheep is an example of polar overdominance inheritance, an unusual mode of inheritance. To investigate the underlying molecular mechanism, we profiled the expression of the genes located in the Delta-like 1 homolog (*Dlk1*)–type III iodothyronine deiodinase (*Dio3*) imprinting region in mice. We found that the transcripts of the microRNA (miR) 379/miR-544 cluster were highly expressed in neonatal muscle and paralleled the expression of the *Dlk1*. We then determined the in vivo role of the miR-379/miR-544 cluster by establishing a mouse line in which the cluster was ablated. The maternal heterozygotes of young mutant mice displayed a hypertrophic tibialis anterior muscle, extensor digitorum longus muscle, gastrocnemius muscle, and gluteus maximus muscle and elevated expression of the DLK1 protein. Reduced expression of DLK1 was mediated by miR-329, a member of this cluster. Our results suggest that maternal expression of the imprinted miR-379/miR-544 cluster regulates paternal expression of the *Dlk1* gene in mice. We therefore propose a miR-based molecular working model for polar overdominance inheritance.

muscle hypertrophy | callipyge | DLK1 | miR-379/miR-544 cluster

The callipyge (CLPG) phenotype can be characterized by an increase in muscle mass due to muscular hypertrophy and a unique non-Mendelian mode of inheritance (1–3). CLPG individuals are born with normal muscle histology and develop muscle hypertrophy at ∼1 mo of age. This hypertrophy occurs primarily in the muscles of the pelvic limbs and loin and some muscles in the shoulder, which are enriched with a high proportion of type IIB fast-twitch glycolytic fibers (4). Although the molecular regulation of these hypertrophic processes is yet to be determined, Delta-like 1 homolog (DLK1) is found to be the causative protein (5–10). The unique mode of inheritance of the CLPG phenotype has attracted a great deal of attention within the scientific community. The CLPG offspring inherit the phenotype only when the mutated allele comes from the father and the wild-type allele from the mother ($CLPG^{PAT}/+^{MAT}$). $CLPG^{PAT}/CLPG^{MAT}$ offspring exhibit a wild-type phenotype, despite carrying a CLPG mutation on the paternal chromosome. This unusual mode of inheritance led to the development of the genetic concept of polar overdominance (2, 11).

The CLPG mutation has been mapped to the *Dlk1–Dio3* imprinted domain, which spans ∼1 Mb and harbors at least three protein-encoding genes, including *Dlk1*, *Peg11*/*Rtl1*, and *Dio3*, and multiple noncoding RNA genes, including *Gtl2*, *anti-Peg11*/*anti-Rtl1*, *Meg8*, *Mirg*, C/D small nucleolar RNAs (snoRNAs), and microRNA clusters [the microRNA (miR) 379 and miR-127 clusters] (12–14). The coding genes are expressed paternally, whereas the noncoding genes are expressed maternally (15, 16). Further analysis revealed a point mutation (A to G transition) within the intergenic region between the *Dlk1* and *Gtl2* genes of the imprinted *Dlk1–Dio3* region (17, 18), which affects a muscle-specific, long-range *cis*-acting control element (18). The point mutation in the paternal allele up-regulates the transcription of genes including *Dlk1* and *Peg11* in *cis* without altering the imprinting status (19). When this mutation occurs in the maternal allele, it up-regulates the expression of noncoding RNAs in the *Dlk1–Dio3* region. If the point mutation occurs in both the paternal and maternal alleles, it causes no change in DLK1 protein expression (4), which is consistent with the mode of inheritance of the CLPG phenotype. It has been demonstrated that DLK1 protein expression is essential for determining muscle mass (20–24). Thus, a hypothesis predicting that maternal noncoding RNA might act as a negative regulator of DLK1 expression has been put forth; however, this hypothesis lacks evidence (25). In this study, we found that the miR-379/miR-544 cluster was dynamically expressed in embryonic and young mice, and this expression paralleled the expression pattern of *Dlk1*. Due to the high conservation of the imprinted *Dlk1–Dio3* region across species (26), we predict that the miR-379/miR-544 cluster might negatively regulate DLK1 protein expression. To test this hypothesis, we deleted this cluster in mice and analyzed its role in skeletal muscle development. As we expected, deletion of the miR-379/miR-544 cluster caused CLPG-like muscular hypertrophy, along with elevated expression of the DLK1 protein, suggesting an essential role of this cluster in muscle growth in young animals. Thus, our results in mice suggest a molecular mechanism for CLPG polar overdominance.

Results

Characteristics of the Expression of the miR-379/miR-544 Cluster in Postnatal Skeletal Muscle. The miR-379/miR-544 cluster is located within the imprinted *Dlk1–Dio3* region, which encompasses the CLPG locus, *Dlk1*, *Gtl2*, anti-*Rtl1*, *Rian*, and *Mirg* (Fig. 1*A*). To understand the role of the miR-379/miR-544 cluster, we measured the expression pattern of its precursor transcript containing all miRs. In adult mice, the primary transcript of the miR-379/miR-544 cluster

Significance

The polar overdominance inheritance of callipyge sheep is an unusual mode of non-Mendelian inheritance. We established a mouse line with deletion of the microRNA (miR) 379/miR-544 cluster and assessed the role of this cluster in the inheritance. Our results showed that the maternally expressed miR-379/miR-544 cluster might regulate skeletal muscle growth through the imprinted Delta-like 1 homolog (*Dlk1*) gene. This report revealed a molecular mechanism of the polar overdominance inheritance.

Author contributions: Y.-Q.G., H.-Q.C., and M.-S.Z. designed research; Y.-Q.G., X.C., P.W., and L.L. performed research; W.Z., C.C., C.-P.C., T.T., J.S., Y.-Y.Z., J.D., C.-J.L., Z.-J.G., and X.G. contributed new reagents/analytic tools; Y.-Q.G., X.C., H.-Q.C., and M.-S.Z. analyzed data; and Y.-Q.G., H.-Q.C., and M.-S.Z. wrote the paper.

The authors declare no conflict of interest.

This article is a PNAS Direct Submission.

[1]Y.-Q.G. and X.C. contributed equally to this work.

[2]To whom correspondence should be addressed. Email: zhums@nju.edu.cn.

This article contains supporting information online at www.pnas.org/lookup/suppl/doi:10.1073/pnas.1511448112/-/DCSupplemental.

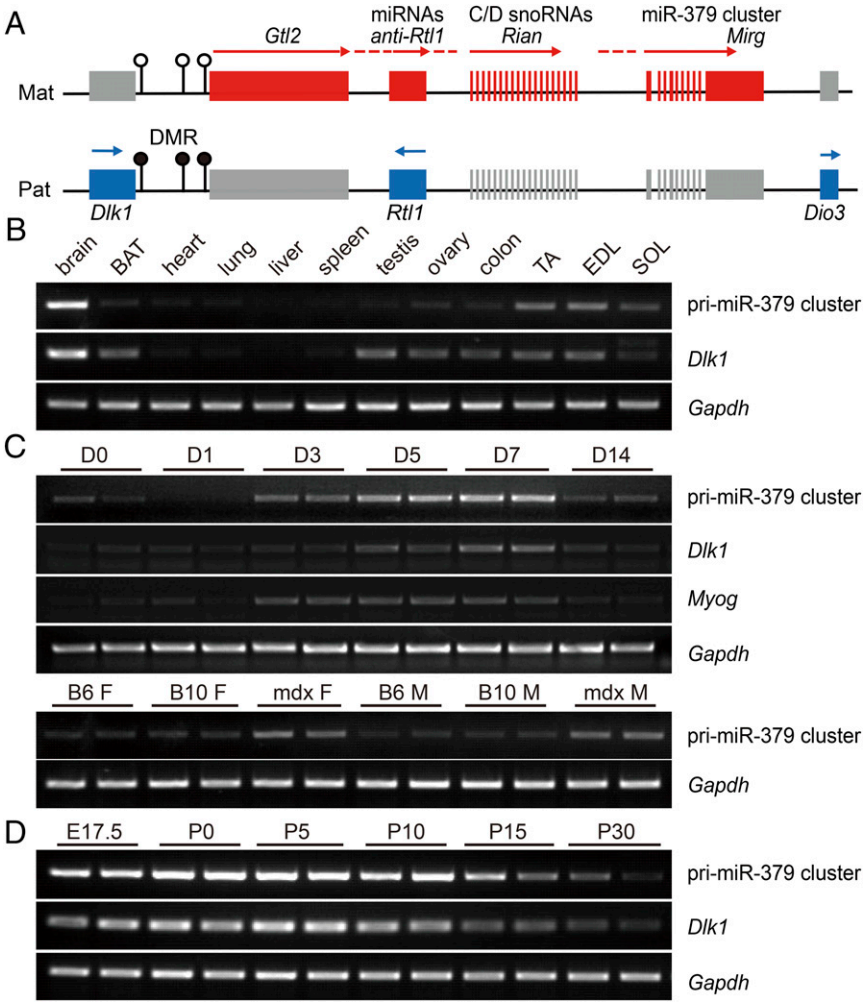

Fig. 1. Spatiotemporal expression pattern of the pri–miR-379/miR-544 cluster. (*A*) Schematic representation of the imprinted *Dlk1–Dio3* region in the mouse distal 12 domain (human 14q32). The protein-coding and long noncoding genes are indicated with squares. SnoRNA and miRNA genes are indicated with vertical threads. Ig-DMR is indicated with filled and open lollipops, representing a methylated or unmethylated status, respectively. Mat, maternal chromosome; Pat, paternal chromosome. (*B*) Expression patterns of the pri–miR-379/miR-544 cluster and *Dlk1* in several tissues in adult mice, assayed via RT-PCR. BAT, brown adipose tissues; EDL, extensor digitorum longus muscle; SOL, soleus muscle; TA, tibialis anterior muscle. (*C*) Expression pattern of the pri–miR-379/miR-544 cluster and DLK1 in adult TA muscle during muscle regeneration (*Upper*) and that in adult mdx mice muscle (*Lower*), assayed via RT-PCR. B6, C57BL/6; B10, C57BL/10; D0 to D14, days post-CTX injection; F, female; M, male. (*D*) Expression patterns of the pri–miR-379/miR-544 cluster and DLK1 in GAST muscles at embryonic, neonatal, and adult stages.

was enriched in the brain but not in skeletal muscles (Fig. 1*B*). However, its expression level was increasingly elevated after treating the muscle with cardiotoxin (CTX), a toxin that induces muscle injury and regeneration (27). Additionally, the expression of this cluster was also up-regulated in *mdx* mice, a disease model of muscular dystrophy characterized by spontaneous necrosis and regeneration (Fig. 1*C*). This expression pattern implies an essential role of this cluster in muscular development/differentiation. We then measured the transcript levels of the miR-379/miR-544 cluster in embryonic and postnatal skeletal muscles and observed higher expression of the miR-379/miR-544 cluster transcripts during embryonic and perinatal stages, whereas lower expression was observed in adult tissues (Fig. 1*D*). As the second peak of skeletal muscle growth occurs during the postnatal stage (28), this observation suggests that the miR-379/miR-544 cluster may play a role in skeletal muscle growth. Because *Dlk1* expression is elevated in CLPG phenotype muscle, which is attributable to an increase in muscle mass, we measured *Dlk1* mRNA at corresponding time points. The results showed dynamic expression of *Dlk1* that paralleled that of the miR-379/miR-544 cluster (Fig. 1 *B–D*). Such an expression pattern implies a regulation of the expression of *Dlk1* by the miR-379/miR-544 cluster.

Ablation of the Expression of the miR-379/miR-544 Cluster in Mice. To investigate the role of the miR-379/miR-544 cluster in vivo, we established a knockout (KO) mouse line. The detailed scheme is presented in Fig. 2*A*. We introduced three *lox*P sites into the loci via homologous recombination through a targeting vector. The third *lox*P site inserted in the middle of the miR-379/miR-544 cluster (miR-379cl) was used for improving deletion efficiency. The chimeric founders were generated through ES electroporation and microinjection. The floxed allele was confirmed by Southern blot analysis (Fig. 2*B*). The floxed mice (*miR-379cl* $^{flox/flox}$) were crossed with EIIa-Cre mice, and their offspring (B6129SF1) were subsequently back-crossed with C57BL/6 mice for more than 10 generations. The genotypes of the resultant mice (C57BL/6) harboring a heterozygous (*miR-379cl*$^{+/-}$) or homozygous deletion (*miR-379cl*$^{-/-}$) were confirmed via Southern blot analysis (Fig. 2*B*) and PCR (Fig. 2*C*). Because the miR-379/miR-544 cluster is located in an imprinting region where only the maternally inherited allele is competent for transcription (29), we bred two extra lines of mice. In these two lines, mice with paternal inheritance of the targeted deletion (paternal KO, P-KO) were established by crossing wild-type C57BL/6 females with heterozygous males (*miR-379cl*$^{+/-}$), whereas mice with maternal inheritance of the targeted deletion (maternal KO, M-KO) were obtained by crossing wild-type C57BL/6 males with heterozygous females (*miR-379cl*$^{+/-}$). RT-PCR analysis showed that P-KO muscle expressed a comparable level of the miR-379/miR-544 cluster transcripts to wild-type muscle, whereas M-KO muscle did not (Fig. 2*D*).

The KO, M-KO, and P-KO pups were born in the expected Mendelian ratios and were viable, appeared normal in size, and reached adulthood without any gross physical abnormalities. All of the adult mice exhibited similar body weights, food intake, and other physiological activities (Figs. S1 and S2). At necropsy, the entire digestive tract, brain, kidneys, lungs, heart, and other organs appeared normal.

Maternal Deletion of the miR-379/miR-544 Cluster Leads to Fast-Twitch Muscle Hypertrophy in Neonatal Mice. Similar to total KO,

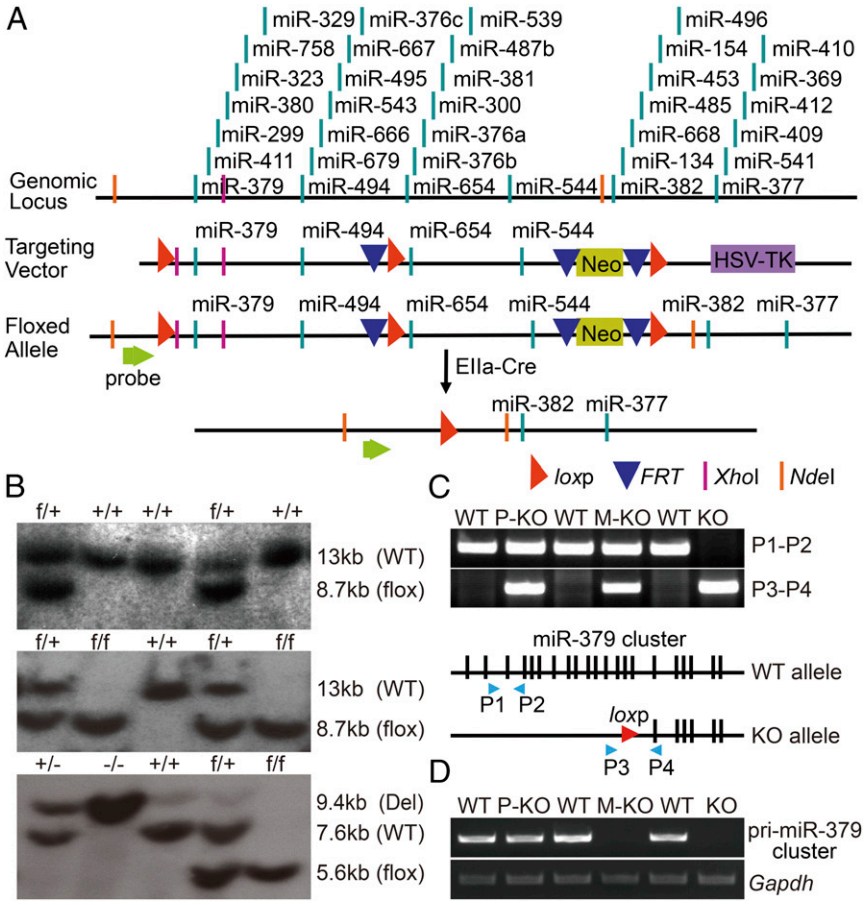

Fig. 2. Generation and confirmation of miR-379/miR-544 cluster null mice. (*A*) Schematic representation of the miR-379/miR-544 flox strategy. Three *lox*P sites were inserted into the genomic DNA. The first *lox*P site was targeted upstream of miR-379, the second *lox*P site was inserted upstream of mir-376c, and the third *lox*P site, with a PGK-Neo cassette, was introduced downstream of miR-544. The first *lox*P cassette contained an XhoI site (blocks in red) designed for Southern blot analysis. The floxed allele formed after homologous recombination in ES cells. Mice containing the floxed allele were crossed with EIIa-Cre mice to generate the miR-379/miR-544 cluster null allele. (*B*, *Top*) Southern blot analysis of miR-379cl floxed ES cells for blastocyst injection. Genomic DNA was digested with BamHI and hybridized with a P^{32}-labeled probe. The 13-kb and 8.7-kb bands represent floxed and wild-type alleles, respectively. (*Middle*) Southern blot analysis of miR-379cl floxed mice used for crosses. (*Bottom*) Southern blot analysis of miR-379cl floxed and miR-379cl null mice. Genomic DNA was digested with XhoI and NdeI. The 9.4-kb, 7.6-kb, and 5.6-kb bands represent the deleted, floxed, and wild-type alleles, respectively. (*C*) Genotype analysis of wild-type mice, heterozygotes, and homozygotes. The P1–P2 primer pair was used to detect the wild-type allele, whereas the P3–P4 primer pair was used for the miR-379cl null allele. (*D*) RT-PCR analysis of the expression level of the pri–miR-379/miR-544 cluster in the skeletal muscles of wild-type mice, M-KO heterozygotes, P-KO heterozygotes, and homozygotes (KO).

M-KO mice showed a normal body size, color, and fur appearance (Fig. 3*A*). The body weight of the M-KO mice was similar to that of wild-type C57BL/6 control mice (Fig. 3*B*). We examined the fat contents of the mutant mice using a PIXImus small-animal dual-energy X-ray absorptiometry (DEXA) system (GE). Among all of the mouse groups, the percentages of fat over body weight were comparable (WT, 22.38 ± 0.81% vs. M-KO, 22.00 ± 0.65%, P10; WT, 19.04 ± 0.47% vs. M-KO, 18.74 ± 1.14%, P20; WT, 18.30 ± 0.83% vs. M-KO, 18.08 ± 0.84%, P30; $P > 0.05$) (Fig. 3*C*). We also examined the muscle mass and histology of individual muscles from the mutant mice. Interestingly, the M-KO mice exhibited significantly larger fast-twitch muscles at P10, including the gastrocnemius (GAST) muscle (WT, 12.18 ± 0.3559 mg vs. M-KO, 13.73 ± 0.4223 mg, $P < 0.001$), tibialis anterior (TA) muscle (WT, 5.175 ± 0.1603 mg vs. M-KO, 5.645 ± 0.1542 mg, $P < 0.01$), and gluteus maximus (GM) muscle (WT, 9.355 ± 0.4444 mg vs. M-KO, 10.28 ± 0.4285 mg, $P < 0.01$) (Fig. 3 *D* and *E*), whereas they displayed a slightly smaller soleus (slow-twitch muscle) (WT, 1.443 ± 0.04680 mg vs. M-KO, 1.354 ± 0.03656 mg, $P < 0.05$). We also analyzed P-KO mice, which expressed the maternal miR-379/miR-544 cluster at a normal level. The P-KO and wild-type mice exhibited a comparable muscle mass (Fig. 3*F*). However, at adulthood (>3 wk), the M-KO mice showed no increase in these fast-twitch muscles (Fig. 3*G*). Fiber typing of the M-KO GAST muscle with MyHCI- and MyHCIIB-specific antibodies showed an increase in type IIB fibers (wild-type, 64.75 ± 1.119% vs. M-KO, 69.14 ± 1.946%, $P < 0.05$) and a decrease in type I fibers (wild-type, 4.347 ± 0.3102% vs. M-KO, 3.559 ± 0.2066%, $P < 0.01$) (Fig. 3 *H* and *I*). The average area of type IIB myofibers in the M-KO GAST muscle increased by ∼17.5 ± 6.264% (Fig. 3 *H* and *I*). Further analysis showed that type IIB myofibers of WT mice were primarily enriched in small fibers (<500 μm^2), whereas those of M-KO mice were enriched in large fibers (>500 μm^2) (Fig. S3). Apparently, the hypertrophy caused by miR-379/miR-544 deletion occurs with more glycolytic fibers in a similar manner of CLPG hypertrophy. This result shows that ablation of the maternal miR-379/miR-544 cluster transcript leads to hypertrophy of neonatal fast-twitch muscle.

Maternal Ablation of the miR-379/miR-544 Cluster Leads to Elevated Expression of the DLK1 Protein. Multiple lines of evidence suggest that the over growth of muscle mass observed in the CLPG phenotype may result from elevated expression of the DLK1 protein (4, 8, 30). We therefore measured *Dlk1* mRNA levels in the GAST muscles of the mutant mice. In adult M-KO mice, the level of the DLK1 protein was low, whereas it was high in neonatal (P0–P10) mice (Fig. 1*D*). Quantitation showed that DLK1 protein expression was increased by ∼1.6-fold in neonatal M-KO mice compared with the wild-type controls ($P < 0.001$) (Fig. 4 *A* and *B*).

As expected, no apparent difference was observed in P-KO mice ($P > 0.05$) (Fig. 4 *D* and *E*). This expression pattern is consistent with that of miR-379/miR-544 expression. We also measured the expression level of *Dlk1* mRNA in the muscles of WT mice and M-KO and P-KO littermates, and no differences were observed (Fig. 4 *C* and *F*). This inconsistent expression of *Dlk1* mRNA and the DLK1 protein implies the occurrence of posttranscriptional regulation of the *Dlk1* gene in muscle.

There is evidence showing that DLK1 may be involved in IGF1 signaling and in muscle growth through Akt phosphorylation (22, 31–33). We measured Akt phosphorylation in hypertrophic muscles. As expected, the muscle tissue of M-KO mice showed a high level of Akt phosphorylation compared with that of WT mice (Fig. S4).

We also measured *Rtl1*/RTL1 (also *Peg11*/PEG11) expression in the muscle tissues from M-KO, P-KO, and WT mice. The result showed that both *Rtl1* mRNA and RTL1 protein expressions were comparable among these groups ($P > 0.05$) (Fig. S5 *A*–*C*).

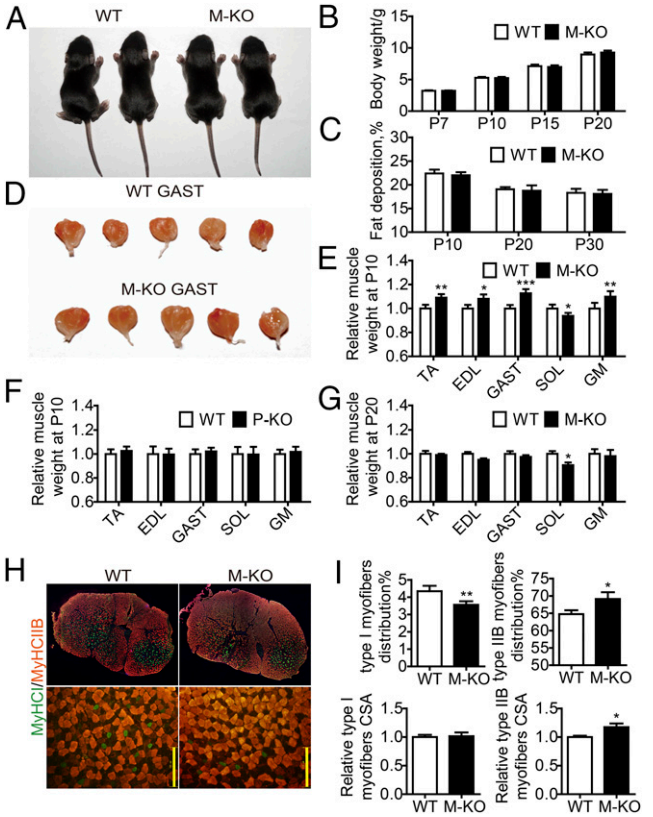

Fig. 3. Maternal deletion of the miR-379/miR-544 cluster leads to neonatal fast-twitch muscle hypertrophy. (*A*) Appearance of WT and M-KO mice at P10. (*B*) Body weight measured before weaning (n = 23–34). (*C*) Fat deposition measured with a PIXImus small-animal DEXA system (n = 5–6). (*D*) General appearance of GAST muscles of WT and M-KO mice at P10. (*E*) Wet muscle weight of WT and M-KO mice at P10 (n = 33–40). (*F*) Wet muscle weight of WT and P-KO mice at P10 (n = 19–24). (*G*) Wet muscle weight of WT and M-KO mice at P20 (n = 8). (*H*) Immunofluorescence staining of fast type IIB and slow type I myofibers of GAST muscles from WT and M-KO mice at P10. (Scale bar, 125 μm.) (*I*, *Top*) The percentage of type I and type IIB myofibers of GAST muscles of M-KO mice and WT mice (n = 5). (*Bottom*) The relative CSA of type I and type IIB myofibers of GAST muscle of M-KO mice and WT mice (n = 6). P10, postnatal day 10. *P < 0.05; **P < 0.01; ***P < 0.001 (Student's t test).

MiR-329 Mediates DLK1 Expression. The inconsistent expression of *Dlk1* mRNA and protein described above suggests that *Dlk1* expression may be regulated by miR. We therefore screened miRs with the potential to bind to the *Dlk1* 3′UTR using bioinformatics software (www.targetscan.org). The predicted candidates included miR-667, 329, 539, 679, and 544 (Fig. 5*A*). We constructed a luciferase reporter by inserting a *Dlk1* 3′UTR fragment downstream of the luciferase gene. The 3′UTR sequence was achieved from National Center for Biotechnology Information (NCBI) resources (gene ID 13386). The luciferase activity of HEK293T cells cotransfected with the miRs was measured. Cotransfection with the miR-329 expression plasmid resulted in significantly lower luciferase activity (~50%) than was observed in the controls (Fig. 5 *B*–*D*), but no change was detected for the other miRs (P > 0.05) (Fig. 5*C*). Mutation of the miR-329 recognition site abolished this inhibitory effect (Fig. 5*E*). We also transfected luciferase reporters as well as miR-329 mimics or scramble miRNA obtaining similar results (Fig. S6 *A* and *B*). To further validate the inhibitory effect of miR-329 on the endogenous *Dlk1* gene, we used C2C12 myoblast cells expressing the native DLK1 protein (24). Western blot analysis showed that the introduction of miR-329 resulted in a ~35% reduction of DLK1 protein levels (64.8 ± 8.1%, P < 0.05), whereas a miR-329 inhibitor led to a ~20% increase of DLK1 protein levels (P > 0.05) (Fig. 5 *F* and *G*). We also tested the in vivo effect of miR-329 on DLK1 expression by intramuscular injection with miRNA agomirs to pairs of hind limbs of M-KO mice. The result showed that injection of miR-329 agomirs led to a significant reduction of DLK1 protein by 22.44 ± 7.336% in comparison with agomir negative control (P < 0.05, n = 4) (Fig. 5*H*). This result shows that Dlk1 may be targeted by miR-329. Because Dlk1 mRNA level was not altered in the KO mice, miR-329 appears to regulate DLK1 expression in a translational inhibition rather than an mRNA stabilization manner (34, 35).

Discussion

CLPG polar overdominance represents a unique mode of inheritance, and its underlying molecular mechanism is therefore of great interest to investigators. The characteristic molecular events of this genetic process include paternal overexpression of DLK1 and PEG11/RTL1 and normal maternal expression of *Gtl2*, *Rian*, *anti-Peg11*, and miRs (19). The prevalent working model for polar overdominance predicts that maternal noncoding RNA within the *Dlk1–Dio3* imprinting region may serve as a *trans*-regulator of DLK1 expression, thereby causing the CLPG phenotype (4). Thus, elucidation of the role of noncoding RNA in the regulation of DLK1 expression and muscle growth is critical. In this study, we assessed the role of the miR-379/miR-544 cluster using a murine KO line. The mutants displayed increases in TA, EDL, GAST, and GM muscle mass and increased expression of the DLK1 protein, as observed in CLPG sheep (4). Accordingly, the activation of Akt signaling was also consistently intensified when DLK1 expression was increased. Among the members of this cluster, miR-329 can directly inhibit the translation of the DLK1 protein by binding to the 3′UTR of *Dlk1* mRNA. These results clearly suggest that this miR cluster, which lies within the *Dlk1–Dio3* imprinting region, may serve as a negative regulator of DLK1 expression. Due to the featured expression pattern of PEG11/RTL1 protein in the CLPG sheep, *Peg11*/*Rtl1* is considered a candidate gene driving the CLPG muscle hypertrophy also (6, 8, 13, 36, 37). We did not observe an apparent change of its expression in the KO mice, implying no involvement of PEG1/RTL1 in the hypertrophic phenotypes in our KO mice. We therefore propose a working molecular model for the polar overdominant inheritance of CLPG phenotypes (Fig. 6). In this model, a maternal CLPG heterozygote expresses a high level of the miR-379/miR-544 cluster from the $CLPG^{MAT}$ allele, whereas the wild-type paternal allele results in expression of DLK1 at a normal level. Thus, no CLPG hypertrophy occurs in wild-type animals. The paternal CLPG heterozygote expresses a high level of DLK1 from the

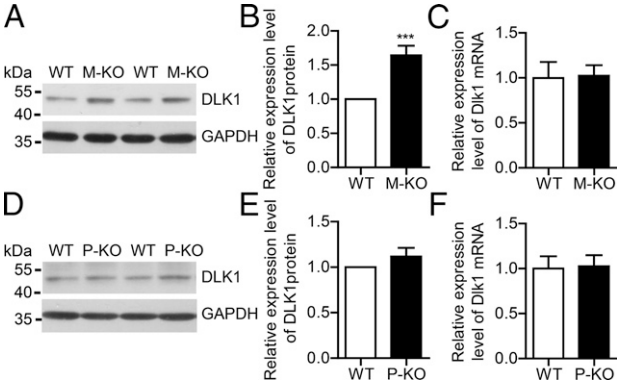

Fig. 4. Maternally expressed miR-379/miR-544 may participate in the post-transcriptional regulation of DLK1. (*A*) Representative Western blot analysis of GAST muscle from neonates shows up-regulation of DLK1 protein expression in M-KO mice. The size of the DLK1 protein band is ~50 kDa. (*B*) Quantification analysis of all of the Western blot results done (n = 20). (*C*) Quantitative RT-PCR analysis of the GM muscle shows comparable *Dlk1* mRNA levels in WT and MKO mice. (*D*) Representative Western blot analysis of the GAST muscle of neonates shows comparable DLK1 protein levels between WT and PKO mice. (*E*) Quantitation of all of the Western blot analyses done (n = 7). (*F*) Quantitative RT-PCR analysis shows comparable *Dlk1* mRNA levels in the GM muscle from WT and PKO mice. ***P < 0.001 (Student's t test).

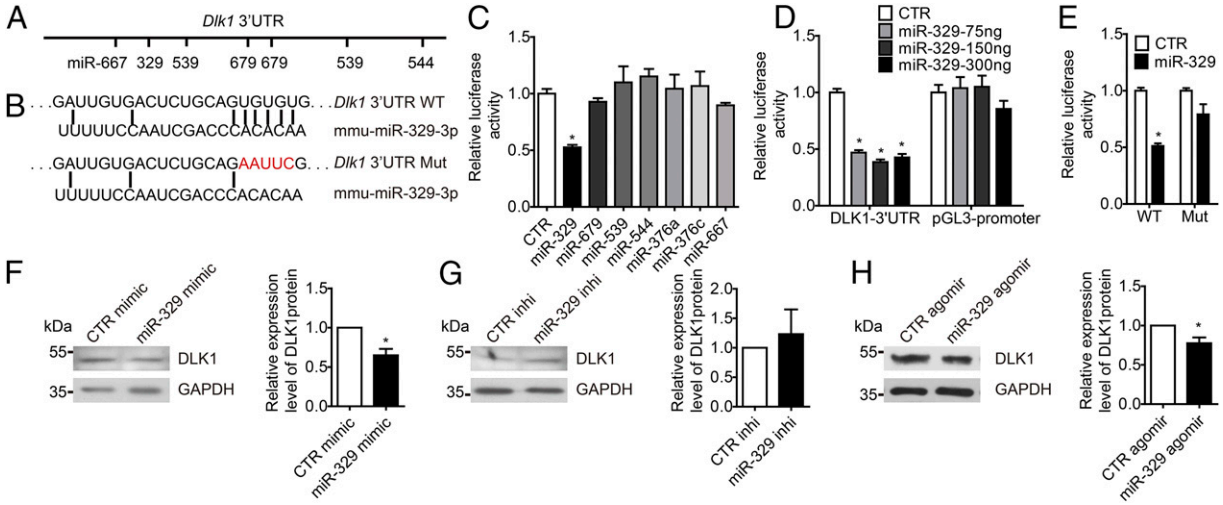

Fig. 5. MiR-329 targets the *Dlk1* gene by interacting with the *Dlk1* 3′UTR. (*A*) Predicted miRs in the miR-379/miR-544 cluster can interact with the 3′UTR of *Dlk1*. (*B*) Schematic representation of potential miR-329 binding sites and the designed mutant sequence in the *Dlk1* 3′UTR. (*C*) Luciferase assays show that, among several candidate miRs, only miR-329 can interact with the *Dlk1*-3′UTR to suppress DLK1 protein expression. (*D*) Luciferase assays show that miR-329 specifically interacts with the *Dlk1* 3′UTR. (*E*) Mutation of potential miR-329 binding sites results in comparable luciferase activity between miR-329 and CTR. (*F* and *G*) Western blot analysis and quantitative results for the DLK1 protein compared with GAPDH when C2C12 cells were transfected with a miR-329 mimic or a miR-329 inhibitor (miR-329 inhi). (*H*) Western blot analysis for the DLK1 protein in the GAST muscles of hind limbs that were injected with CTR agomir or miR-329 agomir ($n = 4$).

$CLPG^{PAT}$ allele, but the wild-type allele results in expression of miR-379/miR-544 at a normal level. Hence, overexpression of the DLK1 protein cannot be sufficiently inhibited, which causes a hypertrophic phenotype. In homozygous individuals, the overexpression of the mir-379/miR-544 cluster is sufficient to inhibit the overexpressed *Dlk1* transcripts, and a normal phenotype is observed.

It has been well established that both young and adult CLPG sheep show an increased muscle mass. However, after deletion of the miR-379/miR-544 cluster, only the young mutant mice showed an increase in muscle mass, whereas the adults displayed no increase. This phenotypic difference may be due to different expression patterns of DLK1. In CLPG sheep, elevated paternal expression of DLK1 caused by a CLPG point mutation persists over the lifespan of the animal (4, 5), whereas in miR-379/miR-544 cluster KO mice, DLK1 is expressed in a physiological manner, showing predominant expression at the neonatal stage and almost no expression during adulthood. Such a transient increase in DLK1 may also be the primary reason why the muscle hypertrophy is relatively small in comparison with CLPG sheep.

Recently, by using an ovine DLK1/Cos1 cell reporter system, Cheng et al. also observed a transinhibition effect of ovine miR-329a (mouse miR-329) on DLK1 expression (38) but suggested that the in vitro effect of miR-329a may not be commensurate with the profound alteration of DLK1 in CLPG sheep in vivo. We here find the ablation of the miRNA cluster containing miR-329 sufficient to cause an increase in DLK expression and a hypertrophic phenotype. With appreciation of this in vivo evidence from the KO mice, we made an alternative conclusion emphasizing the role of the miRNAs in DLK1 regulation.

Interestingly, the KO mice displayed a smaller soleus, which is a slow-twitch muscle. Because this slow-twitch muscle does not express DLK1, we predict that this phenotype may be influenced by other miRs within this cluster through an unknown mechanism. Among the miRs, miR-411 regulates myogenesis by targeting myogenic factors (39), and miR-494 regulates the mitochondrial biogenesis of skeletal muscle by targeting mitochondrial transcription factor A and Forkhead box j3 (40). MiR-329 can inhibit cell proliferation and angiogenesis in vitro by targeting E2F and KDM1A (41, 42). We measured the expression of E2F, KDMIA, and other target proteins of the miR-379/miR-544 cluster in neonatal mice and found no apparent change that was consistent with the expression of the transcripts of this cluster (Fig. S7). Thus, the CLPG-like phenotype of the KO mice is unlikely to be a result of these target proteins.

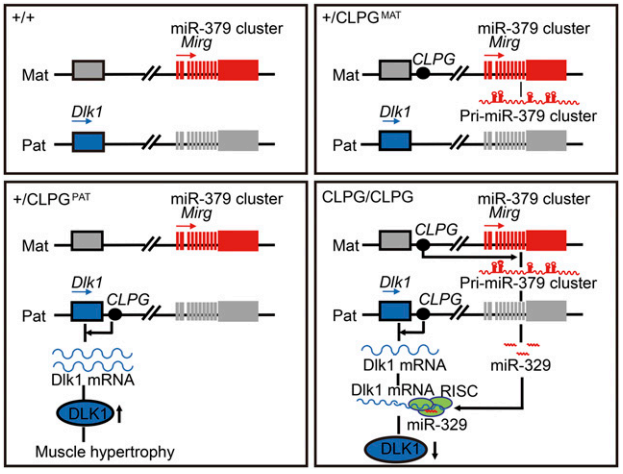

Fig. 6. Working model for CLPG polar overdominant inheritance. The CLPG mutation acts as a long-range control element and enhances the transcript levels of the imprinted genes in cis, without altering their imprinted status. $CLPG^{PAT}$/+ animals exhibit overexpression of DLK1, with normal expression of maternal mi-RNAs, resulting in the CLPG phenotype. $CLPG^{MAT}$/+ animals exhibit overexpression of maternal miRs and normal expression of paternal DLK1, which does not cause the CLPG phenotype. In the CLPG/CLPG animals, paternally overexpressed DLK1 can be posttranscriptionally inhibited by the maternally overexpressed miRs, resulting in no hypertrophy in CLPG/CLPG animals.

Materials and Methods

Detailed methods for all experiments are available in *SI Materials and Methods*.

Generation of miR-379–544 Cluster Null Mice. All animal experiments were performed in an Association for Assessment and Accreditation of Laboratory Animal Care (AAALAC) accredited animal facility. All animal protocols were approved by the Animal Care and Use Committee of the Model Animal Research Center, Nanjing University. The linearized targeting vector was introduced into ES cells (progeny of 129/Sv). The targeted ES cells were microinjected into the blastocysts of C57BL/6 mice to generate chimeric mice. The resultant miR-379cl floxed mice were crossed with EIIa-cre mice to remove

GENETICS

the genomic DNA between the *lox*P sites. The miR-379cl null mice were backcrossed with C57BL/6 mice for more than 10 generations.

Southern Blotting Analysis. Genomic DNA (20 μg) extracted from targeted ES cells or the mice livers were digested with *BamH* I or *NdeI*/*XhoI* and subsequently resolved via electrophoresis. After transferring the DNA to a membrane, followed by UV cross-linking, we hybridized the membrane with a radioactively labeled probe for at least 4 h. Table S1 lists the probe primers used. Autoradiography was performed with Kodak film at –70 °C for 3 d.

Histological Analyses. Fresh skeletal muscle tissues were isolated and immediately frozen in isopentane that had been cooled in liquid nitrogen. MyHC immunofluorescences were conducted as previously described (43). The fiber numbers and cross-sectional areas (CSAs) were then quantified (MyHCI, green; MyHCIIB, red) with Image J (NIH) software. Table S2 lists the primary antibodies used.

RNA Isolation and Quantitative PCR Analysis. Total RNA was extracted from fresh muscle using the RNeasy Fibrous Tissue Mini Kit (Qiagen). The purified RNA samples were reverse-transcribed using the PrimeScript RT Reagent Kit with gDNA Eraser (Takara Bio). Quantitative PCR was performed using the ABI Prism Step-One system with SYBR Green Master Mix reagents (Takara Bio). Fold expression values relative to the wild-type samples within each tissue were calculated using the ΔΔCT method. Table S1 lists the primers used.

Western Blotting Analysis. Tissue lysates (50 μg per lane) were resolved using 12% (wt/vol) SDS/PAGE and then transferred to a PVDF membrane (Bio-Rad). After incubation with the anti-DLK1 (H-118) or (C-19) polyclonal antibody (Santa Cruz) or anti-GAPDH mouse monoclonal antibody (BioWorld) overnight at 4 °C, the blot was probed with HRP-conjugated secondary antibodies. The immunoreactive bands were visualized with ECL (GE Healthcare). Table S2 lists the primary antibodies used.

Luciferase Assays. The *Dlk1* transcript sequences were acquired from NCBI resources (gene ID 13386). The full region of *Dlk1* 3′UTR was amplified from muscle cDNA and subcloned into the pGL3-promoter vector. miR expression plasmids were constructed by subcloning the corresponding miR gene into the pIRES2-EGFP vector. For the dual luciferase reporter analysis, using the Lipomax reagent (Sudgen), HEK293T cells were cotransfected with a DNA mixture containing the miR expression plasmid, luciferase reporters, and a Renilla internal control. At 36 h posttransfection, luciferase activities were measured with the luciferase reporter assay system (Promega Corporation).

Cell Culture and Transfection of a miR Mimic or Inhibitor. Cell culture reagents were purchased from Life Technologies. We used the nucleofection system (Lonza) to transfect miR-329 mimic (100 nM) and miR-329 inhibitor (200 nM) in C2C12 myoblasts. At 36 h posttransfection, the cells were harvested for the detection of DLK1 protein expression.

Intramuscular Injection of miRNA Agomir in Mice. We injected 0.02 mL of 20 μM miR-329 agomir (Ribobio Co., Ltd.) intramuscularly into the right hind limb GAST muscle and CTR agomir into the left hind limb GAST muscle as a control on each P6.5-old WT or M-KO mouse. We collected muscle samples 4 d later.

Statistical Analysis. The data were represented as the mean ± SEM. Two-tailed paired Student's *t* tests were used for comparisons between two groups. A value of $P < 0.05$ was considered statistically significant: $^{*}P < 0.05$; $^{**}P < 0.01$; $^{***}P < 0.001$ (Student's *t* test).

ACKNOWLEDGMENTS. This work was supported by National Key Scientific Research Program of China (973 program) Grants 2014CB964701, 2011CB944104, and 2009CB941602 and National Natural Science Funding of China Grants 31330034, 31371356, and 31272311.

1. Carpenter CE, Rice OD, Cockett NE, Snowder GD (1996) Histology and composition of muscles from normal and callipyge lambs. *J Anim Sci* 74(2):388–393.
2. Cockett NE, et al. (1996) Polar overdominance at the ovine callipyge locus. *Science* 273(5272):236–238.
3. Koohmaraie M, Shackelford SD, Wheeler TL, Lonergan SM, Doumit ME (1995) A muscle hypertrophy condition in lamb (callipyge): Characterization of effects on muscle growth and meat quality traits. *J Anim Sci* 73(12):3596–3607.
4. Davis E, et al. (2004) Ectopic expression of DLK1 protein in skeletal muscle of padumnal heterozygotes causes the callipyge phenotype. *Curr Biol* 14(20):1858–1862.
5. Murphy SK, et al. (2005) Abnormal postnatal maintenance of elevated DLK1 transcript levels in callipyge sheep. *Mamm Genome* 16(3):171–183.
6. Perkins AC, et al. (2006) Postnatal changes in the expression of genes located in the callipyge region in sheep skeletal muscle. *Anim Genet* 37(6):535–542.
7. Cockett NE, et al. (2005) The callipyge mutation and other genes that affect muscle hypertrophy in sheep. *Genet Sel Evol* 37(Suppl 1):S65–S81.
8. Fleming-Waddell JN, et al. (2009) Effect of DLK1 and RTL1 but not MEG3 or MEG8 on muscle gene expression in Callipyge lambs. *PLoS One* 4(10):e7399.
9. Tellam RL, Cockett NE, Vuocolo T, Bidwell CA (2012) Genes contributing to genetic variation of muscling in sheep. *Front Genet* 3:164.
10. Vuocolo T, et al. (2007) Identification of a gene network contributing to hypertrophy in callipyge skeletal muscle. *Physiol Genomics* 28(3):253–272.
11. Georges M, et al. (2004) Toward molecular understanding of polar overdominance at the ovine callipyge locus. *Cold Spring Harb Symp Quant Biol* 69:477–483.
12. Hagan JP, O'Neill BL, Stewart CL, Kozlov SV, Croce CM (2009) At least ten genes define the imprinted Dlk1-Dio3 cluster on mouse chromosome 12qF1. *PLoS One* 4(2):e4352.
13. Seitz H, et al. (2003) Imprinted microRNA genes transcribed antisense to a reciprocally imprinted retrotransposon-like gene. *Nat Genet* 34(3):261–262.
14. Hatada I, et al. (2001) Identification of a new imprinted gene, Rian, on mouse chromosome 12 by fluorescent differential display screening. *J Biochem* 130(2):187–190.
15. Lin SP, et al. (2003) Asymmetric regulation of imprinting on the maternal and paternal chromosomes at the Dlk1-Gtl2 imprinted cluster on mouse chromosome 12. *Nat Genet* 35(1):97–102.
16. da Rocha ST, Edwards CA, Ito M, Ogata T, Ferguson-Smith AC (2008) Genomic imprinting at the mammalian Dlk1-Dio3 domain. *Trends Genet* 24(6):306–316.
17. Freking BA, et al. (2002) Identification of the single base change causing the callipyge muscle hypertrophy phenotype, the only known example of polar overdominance in mammals. *Genome Res* 12(10):1496–1506.
18. Charlier C, et al. (2001) The callipyge mutation enhances the expression of coregulated imprinted genes in cis without affecting their imprinting status. *Nat Genet* 27(4):367–369.
19. Takeda H, et al. (2006) The callipyge mutation enhances bidirectional long-range DLK1-GTL2 intergenic transcription in cis. *Proc Natl Acad Sci USA* 103(21):8119–8124.
20. Bi P, Kuang S (2012) Meat Science and Muscle Biology Symposium: Stem cell niche and postnatal muscle growth. *J Anim Sci* 90(3):924–935.
21. Andersen DC, et al. (2013) Dual role of delta-like 1 homolog (DLK1) in skeletal muscle development and adult muscle regeneration. *Development* 140(18):3743–3753.
22. Waddell JN, et al. (2010) Dlk1 is necessary for proper skeletal muscle development and regeneration. *PLoS One* 5(11):e15055.
23. Sun D, Li H, Zolkiewska A (2008) The role of Delta-like 1 shedding in muscle cell self-renewal and differentiation. *J Cell Sci* 121(Pt 22):3815–3823.
24. Shin S, Suh Y, Zerby HN, Lee K (2014) Membrane-bound delta-like 1 homolog (Dlk1) promotes while soluble Dlk1 inhibits myogenesis in C2C12 cells. *FEBS Lett* 588(7):1100–1108.
25. Georges M, Charlier C, Cockett N (2003) The callipyge locus: Evidence for the trans interaction of reciprocally imprinted genes. *Trends Genet* 19(5):248–252.
26. Edwards CA, et al.; SAVOIR consortium (2008) The evolution of the DLK1-DIO3 imprinted domain in mammals. *PLoS Biol* 6(6):e135.
27. Dey BK, Gagan J, Yan Z, Dutta A (2012) miR-26a is required for skeletal muscle differentiation and regeneration in mice. *Genes Dev* 26(19):2180–2191.
28. White RB, Biérinx AS, Gnocchi VF, Zammit PS (2010) Dynamics of muscle fibre growth during postnatal mouse development. *BMC Dev Biol* 10:21.
29. Seitz H, et al. (2004) A large imprinted microRNA gene cluster at the mouse Dlk1-Gtl2 domain. *Genome Res* 14(9):1741–1748.
30. Fleming-Waddell JN, et al. (2007) Analysis of gene expression during the onset of muscle hypertrophy in callipyge lambs. *Anim Genet* 38(1):28–36.
31. Nueda ML, García-Ramírez JJ, Laborda J, Baladrón V (2008) dlk1 specifically interacts with insulin-like growth factor binding protein 1 to modulate adipogenesis of 3T3-L1 cells. *J Mol Biol* 379(3):428–442.
32. Su R, et al. (2014) Association between DLK1 and IGF-I gene expression and meat quality in sheep. *Genet Mol Res* 13(4):10308–10319.
33. Glass DJ (2005) Skeletal muscle hypertrophy and atrophy signaling pathways. *Int J Biochem Cell Biol* 37(10):1974–1984.
34. Ameres SL, Zamore PD (2013) Diversifying microRNA sequence and function. *Nat Rev Mol Cell Biol* 14(8):475–488.
35. Guo H, Ingolia NT, Weissman JS, Bartel DP (2010) Mammalian microRNAs predominantly act to decrease target mRNA levels. *Nature* 466(7308):835–840.
36. Davis E, et al. (2005) RNAi-mediated allelic trans-interaction at the imprinted Rtl1/Peg11 locus. *Curr Biol* 15(8):743–749.
37. Byrne K, et al. (2010) The imprinted retrotransposon-like gene PEG11 (RTL1) is expressed as a full-length protein in skeletal muscle from Callipyge sheep. *PLoS One* 5(1):e8638.
38. Cheng H, et al. (2014) Experimental evaluation does not reveal a direct effect of microRNA from the callipyge locus on DLK1 expression. *BMC Genomics* 15:944.
39. Harafuji N, Schneiderat P, Walter MC, Chen YW (2013) miR-411 is up-regulated in FSHD myoblasts and suppresses myogenic factors. *Orphanet J Rare Dis* 8:55.
40. Yamamoto H, et al. (2012) MicroRNA-494 regulates mitochondrial biogenesis in skeletal muscle through mitochondrial transcription factor A and Forkhead box j3. *Am J Physiol Endocrinol Metab* 303(12):E1419–E1427.
41. Wang P, et al. (2013) MicroRNA 329 suppresses angiogenesis by targeting CD146. *Mol Cell Biol* 33(18):3689–3699.
42. Xiao B, Tan L, He B, Liu Z, Xu R (2013) MiRNA-329 targeting E2F1 inhibits cell proliferation in glioma cells. *J Transl Med* 11:172.
43. Gan Z, et al. (2013) Nuclear receptor/microRNA circuitry links muscle fiber type to energy metabolism. *J Clin Invest* 123(6):2564–2575.